



OPEN

SUBJECT AREAS:

CHEMICAL
ENGINEERING

FUEL CELLS

Received
4 July 2014Accepted
20 November 2014Published
12 December 2014

Correspondence and
requests for materials
should be addressed to
W.C. (wchoi@
postech.edu) or Y.-E.S.
(ysung@snu.ac.kr)

* These authors
contributed equally to
this work.

Inhibition of CO poisoning on Pt catalyst coupled with the reduction of toxic hexavalent chromium in a dual-functional fuel cell

Dong Young Chung^{1,2*}, Hyoung-il Kim^{3*}, Young-Hoon Chung⁴, Myeong Jae Lee^{1,2}, Sung Jong Yoo⁴, Alok D. Bokare³, Wonyong Choi³ & Yung-Eun Sung^{1,2}

¹Center for Nanoparticle Research, Institute for Basic Science (IBS), Seoul 151-742, Republic of Korea, ²School of Chemical and Biological Engineering, Seoul National University, Seoul 151-742, Republic of Korea, ³School of Environmental Science and Engineering, Pohang University of Science and Technology (POSTECH), Pohang 790-784, Republic of Korea, ⁴Fuel cell Research Center, Korea Institute of Science and Technology, 39-1 Hawolgok-dong, Seoul 136-791, Republic of Korea.

We propose a method to enhance the fuel cell efficiency with the simultaneous removal of toxic heavy metal ions. Carbon monoxide (CO), an intermediate of methanol oxidation that is primarily responsible for Pt catalyst deactivation, can be used as an *in-situ* reducing agent for hexavalent chromium (Cr (VI)) with reactivating the CO-poisoned Pt catalyst. Using electro-oxidation measurements, the oxidation of adsorbed CO molecules coupled with the concurrent conversion of Cr (VI) to Cr (III) was confirmed. This concept was also successfully applied to a methanol fuel cell to enhance its performance efficiency and to remove toxic Cr (VI) at the same time.

Low temperature fuel cells such as proton exchange membrane fuel cells (PEMFCs) and direct alcohol fuel cells (DAFCs) are promising energy conversion devices and ongoing research projects for electrical vehicles and portable devices, however, carbon monoxide (CO) and sulfur poisoning deactivate the platinum catalyst utilization^{1,2}. CO poisoning, one of the worst catalyst deactivating processes, is a crucial issue especially for platinum group metal catalysts in direct methanol fuel cells (DMFCs)^{3,4}. During alcohol oxidation, adsorbed CO molecules generated as reaction intermediates hinder the reaction by blocking the active sites. Hence, much effort has been devoted to mitigate CO poisoning. A well-known strategy involves alloying with highly oxophilic materials such as ruthenium and nickel⁵⁻¹⁰. Gasteiger *et al.*, suggest the bifunctional action, which electro-oxidation of adsorbed intermediate species (methanol dehydrogenation fragments) are catalyzed by oxygen species which is adsorbed by the adjacent Ru atom. Easy adsorption of hydroxyl groups (OH_{ad}), which can be generated at more negative potentials, can then help oxidize the adsorbed CO¹¹. An alternative approach applied to mitigate CO poisoning is the atomic ensemble effect, in which the catalyst surface is modified with molecules or other atoms to induce a direct oxidation pathway wherein CO intermediates are not formed at all^{12,13}. However, further improvements and new concepts to address this issue are still required.

Recently, research have been focused on the integration of both environmental and energy issues to present eco-friendly solutions. For example, coupling an energy conversion process with an environmental remediation process can be considered as an ideal approach. One possible strategy is to use environmentally toxic materials or waste materials as energy sources. Elemental sulfur, a byproduct of petroleum refinement, could be used as an active material in lithium battery¹⁴⁻¹⁶, whereas hydrogen production was obtained by photocatalysis or electrolysis of human wastewater^{17,18}. Such systems can simultaneously achieve both energy production and removal of environmental pollutants. This work tried to apply the dual-purpose strategy to fuel cell applications.

Chromium is one of the most harmful heavy metals in the aquatic environment. Among its two major oxidation states (hexavalent [Cr (VI)] and trivalent [Cr (III)])¹⁹, the hexavalent species is toxic and carcinogenic, whereas trivalent chromium is much less toxic and needed even as a micronutrient^{20,21}. Therefore, various physico-chemical and biological methods have been established to convert Cr (VI) to Cr (III)²¹⁻²⁴. While Cr (VI) is a strong oxidant [$E^0(\text{Cr (VI)}/\text{Cr (III)}) = 1.35 \text{ V}_{\text{NHE}}$] that can oxidize numerous inorganic and organic substances with converting itself to Cr (III)^{19,25}, metal nanoparticle synthesis using CO demonstrated the cap-

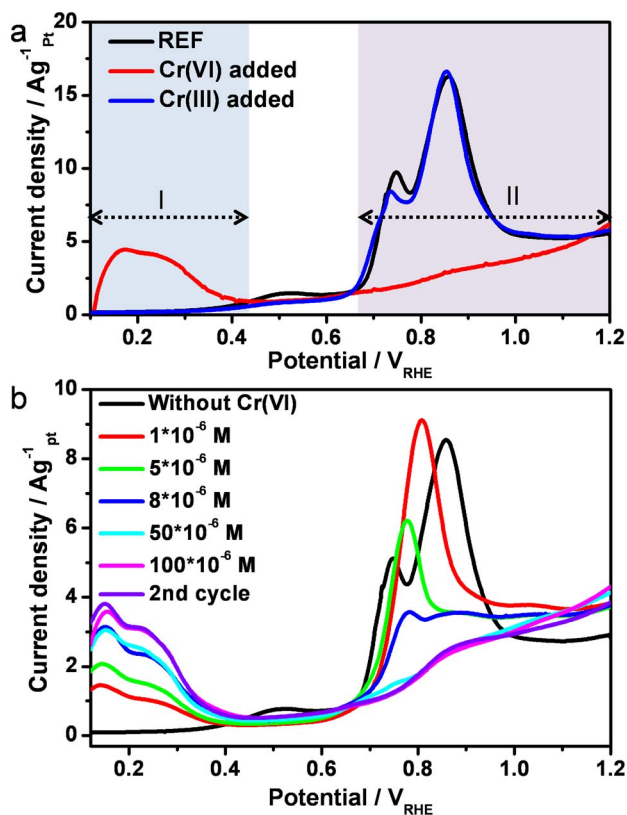


Figure 1 | Cyclic voltammograms analysis of CO electro-oxidation (a) CO electro-oxidation in the absence (REF) and presence of Cr (VI) or Cr (III) (250 μM), and (b) CO electro-oxidation in the presence of different concentrations of Cr (VI).

ability of CO as a reducing agent^{26,27}. Combining the redox properties of Cr (VI) and CO, we suggest a new concept that CO adsorbed on Pt catalyst is oxidized to CO_2 by the reduction of Cr (VI) to Cr (III), which achieves the enhancement of fuel cell efficiency and the removal of toxic pollutants simultaneously. We confirmed this effect in a direct methanol fuel cell (DMFC) and proposed a model fuel cell system that utilizes environmental pollutants as a reagent inhibiting the catalyst deactivation.

Results

To test the reaction between CO and Cr (VI), electro-oxidation of CO was investigated in the absence and presence of Cr (VI) and their detail experimental conditions are given in Supporting Information and Figure S1a. Before the CO adsorption, pre-cycling was performed until a stable cyclic voltammogram was obtained under Ar purging. CO gas was then introduced at a set potential of $0.05 V_{\text{RHE}}$ to adsorb CO on the Pt surface. After 5 min, the CO molecules were fully adsorbed on Pt and before CO oxidation, both catalysts for the absence and presence of Cr (VI) had the similar amount of CO adsorption, as shown in Figure S1b. Non-adsorbed CO molecules remaining in the electrolyte were removed by Ar purging for 20 min. After purging, the working electrode was immersed in a solution containing hexavalent chromium and perchloric acid. A control solution containing only perchloric acid was also tested as a reference. In the reference case (electrode immersed in perchloric acid only), the CO oxidation peaks were observed from 0.6 to $1.2 V_{\text{RHE}}$ in the first cycle (Figure 1a, region II). However, in the presence of Cr (VI), the CO oxidation peaks were completely absent, which means that adsorbed CO was removed during the immersion of Cr (VI) solution. The desorption of hydrogen is also clearly visible. (H_{upd}

(underpotential deposition of proton) represents the electro-deposition of proton at a less negative potential than the reduction potential of proton, region I). The overall reaction scheme is shown as Figure 2.

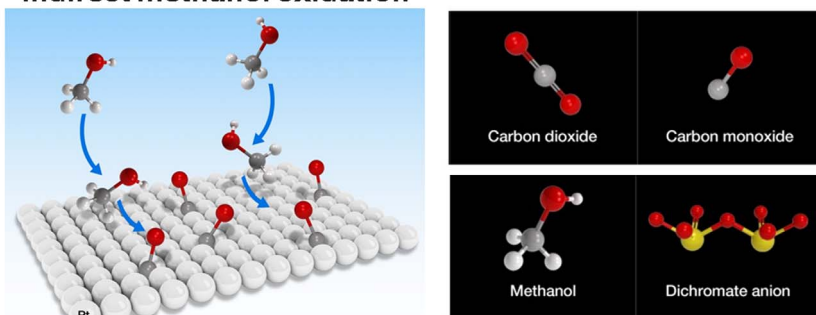
This dual conversion of toxic-hexavalent chromium and CO was applied to DMFC, which is a promising renewable energy conversion system²⁸. The methanol (fuel) oxidation mechanism on the Pt anode has two pathways^{29,30}. The first is a direct mechanism with straightforward evolution of CO_2 , and the other is an indirect reaction in which CO formation poisons the Pt catalyst surface. Unfortunately, the indirect pathway is dominant in most cases. Adsorbed CO, generated as a byproduct of methanol oxidation, blocks the surface active sites and eventually deactivates the catalyst. If Cr (VI) can oxidize the adsorbed CO, it not only reduces CO poisoning of the DMFC anode but also improves the cathode kinetics^{31,32}. We used Pt nanoparticles deposited on carbon as the catalyst for both anode and cathode. Methanol (1 M) was used as the anode fuel and air was used as the cathode fuel. To confirm the role of the hexavalent chromium in DMFC, Cr (VI) was introduced into the anode cell. The cell performance was evaluated at 70°C and the results are shown in Figure 3a. The cell performance at 70°C was improved in the presence of Cr (VI): both maximum power density and open circuit voltage (OCV) were enhanced. The increase in OCV with Cr(VI) indicates that methanol oxidation occurs more efficiently at the anode because more free sites are available by the action of Cr(VI) that mitigates CO poisoning. The cell performance was also compared at 85°C with and without Cr (VI) (Figure 3b). Because the adsorption of CO is weaker at higher temperature, CO poisoning effect is much less at higher temperature³³.

As a result, the presence of Cr (VI) had insignificant effect on the DMFC performance at 85°C unlike the case of 70°C . In the presence of Cr (VI), the maximum power density at 70°C was increased by 20% whereas that at 85°C was not influenced at all (Figure 3c). Electrochemical impedance spectroscopy (EIS) showed that the charge transfer resistance decreased upon the introduction of Cr (VI) (Figure S2). The main arc represents the charge transfer resistance of both anode and cathode. In the presence of Cr (VI), the charge transfer resistance at 70°C decreased since the number of reaction sites were larger compared to the reference condition. As a result of the redox conversion, the concentration of Cr (VI) in the outlet fuel (*see* Figure S3 for the experimental setup), measured using a modified diphenylcarbazide (DPC) method³⁴, clearly decreased after the anode reaction (Figure 3d).

One possible problem using hexavalent chromium in DMFC is the deactivation of Pt site by the precipitation of Cr (III) as amorphous $\text{Cr}(\text{OH})_x$ on the catalyst surface. To investigate the possible catalyst deactivation by the chromium species, the surface of Pt/C was characterized by XPS after 1 h reaction in the presence of Cr (VI). As shown in Figure S4, the XPS analysis showed no sign of chromium species since the formation of $\text{Cr}(\text{OH})_3$ is not favored at such acidic pH ($\text{pH} < 3$) condition³⁵. In addition, the DMFC efficiency decrease was not observed during 1 h operation. This rules out any possible influence of $\text{Cr}(\text{OH})_x$ on the catalyst passivation. The effect of Cr (VI) addition on DMFC performance was also investigated in more detail by employing chronopotentiometry. In the absence of chromium, the potential decreased gradually, mainly because of CO poisoning. However, when Cr (VI) was added, the potential maintained a nearly constant value up to 10 h because of inhibited CO poisoning (*see* Figure 4a). After 10 h reaction of DMFC, 250 μM of Cr (VI) was almost completely removed with exhibiting first order kinetics ($k_{\text{obs}} = 0.004 \text{ min}^{-1}$) (Figure 4b). It should be noted that the cell voltage started to decrease after 7 h when the concentration of Cr (VI) fell below 50 μM , which suggests the re-accumulation of CO on the Pt surface as Cr (VI) concentration is depleted. This is consistent with the data of Figure 1b wherein the adsorbed CO was not fully removed at $[\text{Cr (VI)}]_0 < 50 \mu\text{M}$.



a Indirect methanol oxidation



b Cleaning process "CO removal"

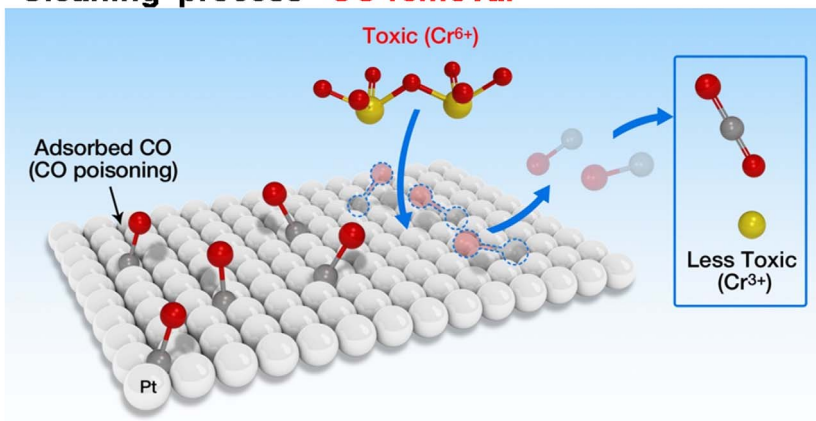


Figure 2 | Schematic diagrams of concepts (a) CO poisoning through indirect methanol oxidation, and (b) proposed cleaning process by introduction of toxic hexavalent chromium ions as "CO scavenger".

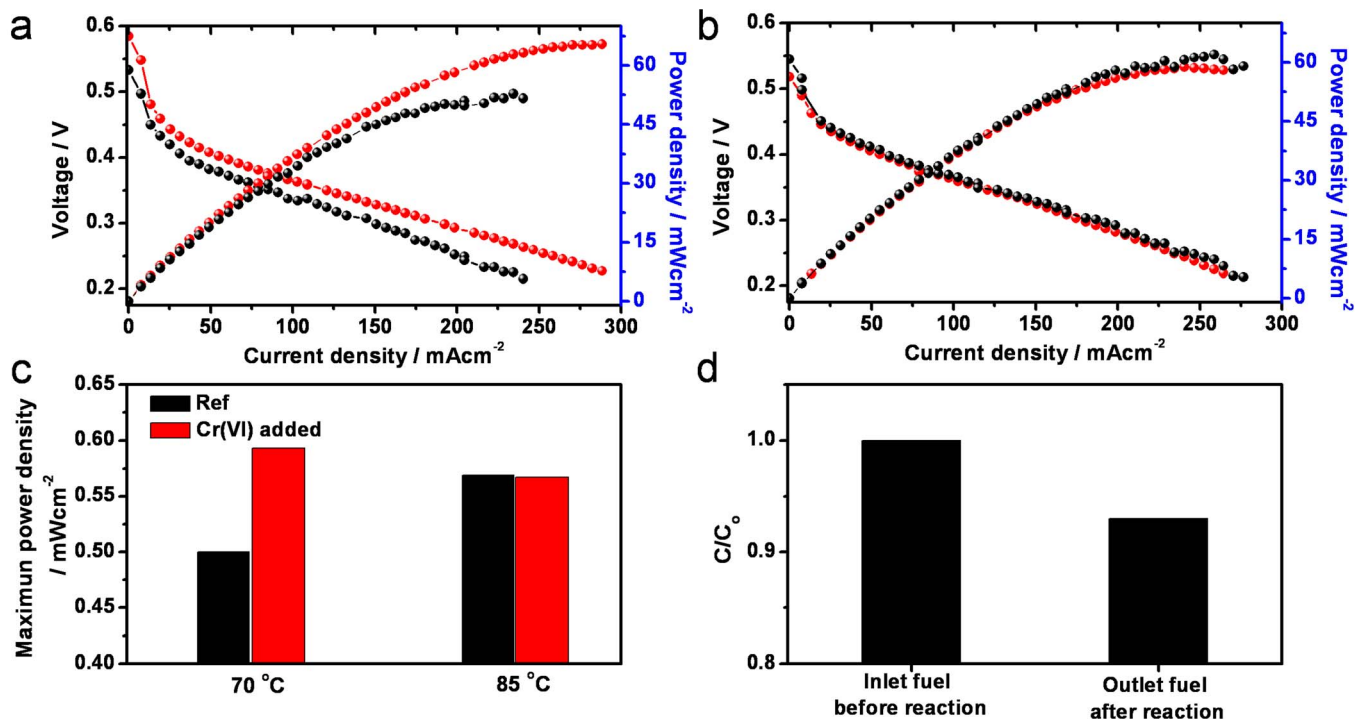


Figure 3 | Performance of DMFC in the absence (black circle) and presence (red circle) of 500 μM Cr (VI) operating at (a) 70°C and (b) 85°C. Panel (c) shows comparison of maximum power densities of DMFC with and without Cr (VI). Panel (d) shows the change of Cr (VI) concentration after the DMFC anode reaction.

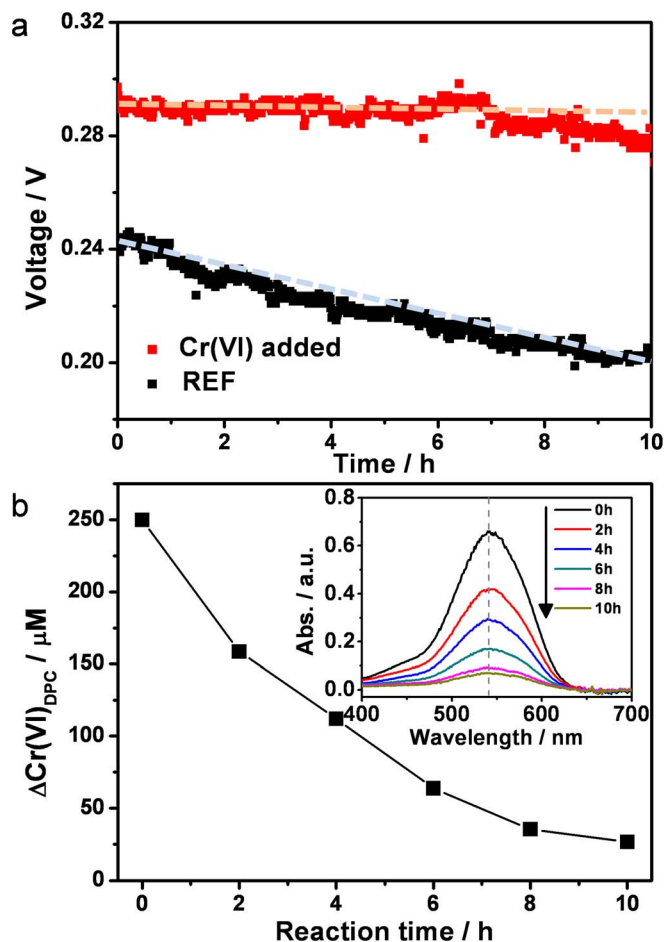


Figure 4 | Chronopotentiometry and Cr (VI) concentration tracking. (a) Chronopotentiometry of DMFC with constant current of 1 A, and (b) time profile of the outlet Cr (VI) concentration measured during chronopotentiometry.

Discussion

The electro-oxidation measurements clearly showed that the adsorbed CO was removed by Cr (VI). Based on the standard reduction potential values for CO_{ad} electro-oxidation coupled with OH_{ad} , $\text{CO}(\text{g})$ oxidation to CO_2 and Cr (VI) reduction and $[E^0(\text{CO}_2/\text{CO}_{\text{ad}} + \text{OH}_{\text{ad}}) = 0.7 \sim 0.8 V_{\text{NHE}}$ (from electrochemical measurements)], $[E^0(\text{CO}_2/\text{CO}) = -0.1 V_{\text{NHE}}$] and $[E^0(\text{Cr}_2\text{O}_7^{2-}/\text{Cr}^{3+}) = 1.35 V_{\text{NHE}}$], the oxidation of CO to CO_2 coupled with the reductive conversion of Cr (VI) to Cr (III) is thermodynamically spontaneous. This redox process achieved not only the cleaning of the Pt electrode surface but also the transformation of toxic Cr (VI) into non-toxic Cr (III). On the other hand, the effect of Cr (III) on the CO oxidation was also investigated as a control experiment. Since the oxidation of CO by Cr (III) is thermochemically non-spontaneous $[E^0(\text{Cr}(\text{III})/\text{Cr}(0)) = -0.74 V_{\text{NHE}}$ and $E^0(\text{Cr}(\text{III})/\text{Cr}(\text{II})) = -0.42 V_{\text{NHE}}$]³⁶, the presence of Cr (III) had no effect on the CO oxidation as shown in Figure 1a. This confirms that the oxidation of CO is facilitated by the electrochemical reduction of Cr (VI). As a result, the removal (oxidation) of CO is enhanced at higher concentration of Cr (VI) with shifting the oxidation peak to the less positive potentials (Figure 1b).

Due to the possible contamination and potential change during the transfer to the Cr (VI) solution through the air, we measured again the electro-oxidation of CO with the addition of Cr (VI) directly to the solution without transfer experiment. Figure S5 shows that the same features were confirmed compared to Figure 1a results. We also checked the open circuit potential (OCP) change after introduction of Cr (VI). The OCP of normal Pt/C electrode was about 0.8

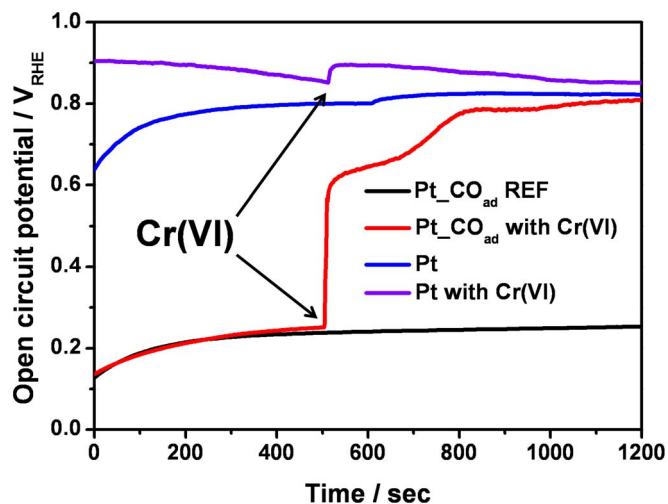


Figure 5 | Open circuit potential (OCP) (black and red lines represent the OCP change on CO adsorbed Pt with and without Cr (VI) addition (at 500 sec), respectively. Blue and purple lines represent the OCP change on bare Pt with and without Cr (VI) addition (at 500 sec), respectively.

V_{RHE} in HClO_4 solution under Ar, (Figure 5, blue). Interestingly, after the CO was adsorbed to the Pt/C surface, the OCP was around 0.25 V_{RHE} (Figure 5, black and red). Considering that the OCP was affected by the Pt surface state and adsorption, the CO adsorption can cover the Pt surface and inhibit adsorption of charged species such as H^+ , OH^- and HClO_4^- . Because the CO was neutral probe³⁷, the OCP values with CO_{ad} were regarded as potential of zero total charge (PZTC), which means that excess charge density plus the charge density transferred during the adsorption equals zero³⁸, and well matched with previous results^{38,39}. After introducing the Cr (VI) solution (Figure 5 red at 500 sec), the OCP was rapidly increased up to 0.6 V_{RHE} and steadily increased to the 0.8 V_{RHE} , which means that Cr (VI) effectively removed the surface CO_{ad} . After the removal of CO in Pt surface, the OCP nearly recovered its original potential (blue and purple). The OCP of Pt without CO adsorption can also slightly affected after Cr (VI) introduction, however the OCP change is negligible which means that addition of $\text{Cr}_2\text{O}_7^{2-}$ anion and Na^+ cation does little affect the OCP. From the OCP measurement and thermodynamic potential view, it is believed that the addition of Cr (VI) can selectively remove CO_{ad} without interfering the electronic property of Pt.

In summary, we herein suggest a novel concept for achieving high fuel cell efficiency and removal of toxic heavy metal ions simultaneously. CO molecules adsorbed on the Pt surface can be used as a reducing agent for Cr (VI), which achieves the dual conversion of Cr (VI) \rightarrow Cr (III) and $\text{CO} \rightarrow \text{CO}_2$. The proposed dual-purpose redox process was confirmed by electrochemical measurements and successfully applied to DMFC, which may serve as a model fuel cell system that utilizes Cr (VI)-contaminated wastewater as an additive in fuel.

Methods

CO electro-oxidation reaction. 5 mg of Pt/C (40 wt.%, Johnson Matthey Co.) was sonicated with DI water, 28.6 μL of Nafion solution (5 wt.%, Aldrich), and 400 μL of 2-propanol (99.9%, Aldrich). After dispersing the ink, 3.5 μL of ink was dropped onto a glassy carbon electrode. All electrochemical measurements were carried out using an Autolab potentiostat (PGSTAT 302N). A standard three electrochemical cell with Pt wire and saturated calomel electrode (SCE) was utilized as a counter and reference electrode, respectively. All potentials were reported with respect to the reversible hydrogen electrode (RHE) using hydrogen oxidation method. In order to get a reproducible data, several potential sweeps between 0.05 V and 1.2 V (vs. RHE) were applied to the electrode under Ar. For CO oxidation experiments, CO was introduced into Ar-purged 0.1 M HClO_4 electrolyte for 12 min at a constant voltage (0.05 V vs. RHE). After saturation of the Pt with CO, excess CO was eliminated by purging with Ar for 30 min and then the electrode was immersed into the HClO_4 (in reference) and



HClO₄ + hexavalent chromium ion (Sodium dichromate dihydrate, Cr₂Na₂O₇·2H₂O, Sigma-Aldrich). The CO oxidation was obtained from 0.05 V to 1.2 V vs. RHE. For control experiment with trivalent chromium, chromium (III) chloride hexahydrate (CrCl₃·6H₂O, Sigma-Aldrich) was used.

DMFC operation. Catalyst ink was prepared from 60 wt.% Pt/C (Johnson Matthey), 5 wt.% Nafion ionomer and isopropyl alcohol. The prepared catalyst ink was blended by ultrasonication. A catalyst coated membrane type of MEA was fabricated by spraying the catalyst ink onto both sides of a Nafion 115 membrane that had been treated with 3 wt.% H₂O₂ solution for 1 h and 0.5 M H₂SO₄ solution for 1 h. Pt loading was 2 mg cm⁻² in the anode and 0.5 mg cm⁻² in the cathode, respectively. 1 M methanol solution was fed into the anode, and air was supplied to the cathode at 70 and 85 °C.

Chronopotentiometry. Chronopotentiometry was measured with 1 A at 70 °C. The concentration of hexavalent chromium ion in the outlet feed was determined by DPC (diphenylcarbazide) method. 1 M methanol solution and 250 μM of hexavalent chromium were fed into the anode with 3 mL min⁻¹ flow rate.

OCP measurement. Open circuit potential (OCP) was measured after CO adsorption. The Cr (VI) solution was introduced after 500 sec. Control experiment was also conducted without CO adsorption.

DPC method. In the modified DPC method, an aliquot of samples was extracted and then diluted with water (total volume of 3 mL). Sequential additions were followed with 0.1 mL of DPC in acetone (2 g L⁻¹) and 0.1 mL of 9 M H₂SO₄. The absorbance of the colored Cr-DPC complex was monitored at 540 nm using a UV/Vis spectrophotometer (Agilent 8453) within 30 min.

- Sung, Y. E., Chrzanowski, W., Zolfaghari, A., Jerkiewicz, G. & Wieckowski, A. Structure of chemisorbed sulfur on a Pt(111) electrode. *J. Am. Chem. Soc.* **119**, 194–200 (1997).
- Jung, N. *et al.* Methanol-tolerant cathode electrode structure composed of heterogeneous composites to overcome methanol crossover effects for direct methanol fuel cell. *Int. J. Hydrogen Energy* **36**, 15731–15738 (2011).
- Cheng, X. *et al.* A review of PEM hydrogen fuel cell contamination: Impacts, mechanisms, and mitigation. *J. Power Sources* **165**, 739–756 (2007).
- Christoffersen, E., Liu, P., Ruban, A., Skriver, H. L. & Nørskov, J. K. Anode materials for low-temperature fuel cells: A density functional theory study. *J. Catal.* **199**, 123–131 (2001).
- Zhao, X. *et al.* Recent advances in catalysts for direct methanol fuel cells. *Energy Environ. Sci.* **4**, 2736–2753 (2011).
- Rossmel, J. *et al.* Bifunctional anode catalysts for direct methanol fuel cells. *Energy Environ. Sci.* **5**, 8335–8342 (2012).
- Park, K. W. *et al.* Chemical and electronic effects of Ni in Pt/Ni and Pt/Ru/Ni alloy nanoparticles in methanol electrooxidation. *J. Phys. Chem. B* **106**, 1869–1877 (2002).
- Park, K. W., Sung, Y. E., Han, S., Yun, Y. & Hyeon, T. Origin of the enhanced catalytic activity of carbon nanocoil-supported PtRu alloy electrocatalysts. *J. Phys. Chem. B* **108**, 939–944 (2004).
- Gasteiger, H. A., Markovic, N., Ross Jr, P. N. & Cairns, E. J. CO electrooxidation on well-characterized Pt-Ru alloys. *J. Phys. Chem.* **98**, 617–625 (1994).
- Gasteiger, H. A., Markovic, N., Ross Jr, P. N. & Cairns, E. J. Methanol electrooxidation on well-characterized Pt-Ru alloys. *J. Phys. Chem.* **97**, 12020–12029 (1993).
- Iwasita, T., Hoster, H., John-Anacker, A., Lin, W. F. & Vielstich, W. Methanol oxidation on PtRu electrodes. Influence of surface structure and Pt-Ru atom distribution. *Langmuir* **16**, 522–529 (2000).
- Cuesta, A. At least three contiguous atoms are necessary for CO formation during methanol electrooxidation on platinum. *J. Am. Chem. Soc.* **128**, 13332–13333 (2006).
- Cuesta, A. Atomic ensemble effects in electrocatalysis: The site-knockout strategy. *ChemPhysChem* **12**, 2375–2385 (2011).
- Ji, X., Lee, K. T. & Nazar, L. F. A highly ordered nanostructured carbon-sulphur cathode for lithium-sulphur batteries. *Nat. Mater.* **8**, 500–506 (2009).
- Chung, W. J. *et al.* The use of elemental sulfur as an alternative feedstock for polymeric materials. *Nat. Chem.* **5**, 518–524 (2013).
- Zhang, S. S. Liquid electrolyte lithium/sulfur battery: Fundamental chemistry, problems, and solutions. *J. Power Sources* **231**, 153–162 (2013).
- Cho, K., Kwon, D. & Hoffmann, M. R. Electrochemical treatment of human waste coupled with molecular hydrogen production. *RSC Advances* **4**, 4596–4608 (2014).
- Cho, K. *et al.* Effects of anodic potential and chloride ion on overall reactivity in electrochemical reactors designed for solar-powered wastewater treatment. *Environ. Sci. Technol.* **48**, 2377–2384 (2014).
- Rai, D., Eary, L. E. & Zachara, J. M. Environmental chemistry of chromium. *Sci. Total Environ.* **86**, 15–23 (1989).
- Wang, W. X., Griscom, S. B. & Fisher, N. S. Bioavailability of Cr(III) and Cr(VI) to marine mussels from solute and particulate pathways. *Environ. Sci. Technol.* **31**, 603–611 (1997).
- Fendorf, S. E. & Li, G. Kinetics of chromate reduction by ferrous iron. *Environ. Sci. Technol.* **30**, 1614–1617 (1996).
- Park, Y. *et al.* Fullerol-titania charge-transfer-mediated photocatalysis working under visible light. *Chem. Eur. J.* **15**, 10843–10850 (2009).
- Kim, S., Yeo, J. & Choi, W. Simultaneous conversion of dye and hexavalent chromium in visible light-illuminated aqueous solution of polyoxometalate as an electron transfer catalyst. *Appl. Catal. B-Environ.* **84**, 148–155 (2008).
- Lovley, D. R. Dissimilatory metal reduction. *Annu. Rev. Microbiol.* **47**, 263–290 (1993).
- Bokare, A. D. & Choi, W. Advanced oxidation process based on the Cr(III)/Cr(VI) redox cycle. *Environ. Sci. Technol.* **45**, 9332–9338 (2011).
- Kang, Y., Ye, X. & Murray, C. B. Size- and shape-selective synthesis of metal nanocrystals and nanowires using CO as a reducing agent. *Angew. Chem. Int. Ed.* **49**, 6156–6159 (2010).
- Wu, J., Gross, A. & Yang, H. Shape and composition-controlled platinum alloy nanocrystals using carbon monoxide as reducing agent. *Nano Lett.* **11**, 798–802 (2011).
- Kamarudin, S. K., Achmad, F. & Daud, W. R. W. Overview on the application of direct methanol fuel cell (DMFC) for portable electronic devices. *Int. J. Hydrogen Energy* **34**, 6902–6916 (2009).
- Iwasita, T. Electrocatalysis of methanol oxidation. *Electrochim. Acta* **47**, 3663–3674 (2002).
- Wasmus, S. & Küver, A. Methanol oxidation and direct methanol fuel cells: A selective review. *J. Electroanal. Chem.* **461**, 14–31 (1999).
- Liu, H. *et al.* A review of anode catalysis in the direct methanol fuel cell. *J. Power Sources* **155**, 95–110 (2006).
- Heinzel, A. & Barragán, V. M. Review of the state-of-the-art of the methanol crossover in direct methanol fuel cells. *J. Power Sources* **84**, 70–74 (1999).
- Li, Q., He, R., Jensen, J. O. & Bjerrum, N. J. Approaches and Recent Development of Polymer Electrolyte Membranes for Fuel Cells Operating above 100 °C. *Chem. Mater.* **15**, 4896–4915 (2003).
- Clesceri, L. S., Greenberg, A. E. & Eaton, A. D. *Standard Methods for the Examination of Water and Wastewater* 20th ed. (APHA American Public Health Association, 1998).
- Bokare, A. D. & Choi, W. Chromate-induced activation of hydrogen peroxide for oxidative degradation of aqueous organic pollutants. *Environ. Sci. Technol.* **44**, 7232–7237 (2010).
- Bard, A. J., Parsons, R. & Jordan, J. *Standard Potentials in Aqueous Solution*. p. 461 (Marcel Dekker, 1985).
- Van Der Vliet, D. F. *et al.* Unique electrochemical adsorption properties of Pt-skin surfaces. *Angew. Chem. Int. Ed.* **51**, 3139–3142 (2012).
- Mayrhofer, K. J. J. *et al.* The impact of geometric and surface electronic properties of Pt-catalysts on the particle size effect in electrocatalysis. *J. Phys. Chem. B* **109**, 14433–14440 (2005).
- Chung, D. Y., Chung, Y. H., Jung, N., Choi, K. H. & Sung, Y. E. Correlation between platinum nanoparticle surface rearrangement induced by heat treatment and activity for an oxygen reduction reaction. *PCCP* **15**, 13658–13663 (2013).

Acknowledgments

This work was supported by IBS-R006-G1, and the Global Frontier R&D Program on Center for Multiscale Energy System funded by the National Research Foundation under the Ministry of Science, ICT & Future, Korea (2011-0031571)

Author contributions

D.Y.C. and H.-i.K. contributed to the design and conduct the experiment and discuss the results with Y.-H.C., M.J.L., S.J.Y. and A.B., D.Y.C., H.-i.K., W.C. and Y.-E.S. contribute to the writing the paper. W.C. and Y.-E.S. contributed to supervising this project. All authors discussed the results and commented on the manuscript.

Additional information

Supplementary information accompanies this paper at <http://www.nature.com/scientificreports>

Competing financial interests: The authors declare no competing financial interests.

How to cite this article: Chung, D.Y. *et al.* Inhibition of CO poisoning on Pt catalyst coupled with the reduction of toxic hexavalent chromium in a dual-functional fuel cell. *Sci. Rep.* **4**, 7450; DOI:10.1038/srep07450 (2014).



This work is licensed under a Creative Commons Attribution-NonCommercial-NoDerivs 4.0 International License. The images or other third party material in this article are included in the article's Creative Commons license, unless indicated otherwise in the credit line; if the material is not included under the Creative Commons license, users will need to obtain permission from the license holder in order to reproduce the material. To view a copy of this license, visit <http://creativecommons.org/licenses/by-nc-nd/4.0/>